Loss of chondroitin 6-*O*-sulfotransferase-1 function results in severe human chondrodysplasia with progressive spinal involvement

Holger Thiele*†, Masahiro Sakano‡, Hiroshi Kitagawa‡, Kazuyuki Sugahara‡, Anna Rajab§, Wolfgang Höhne¶, Heide Ritter*†, Gundula Leschik*, Peter Nürnberg*†, and Stefan Mundlos*‖**

*Institute of Medical Genetics and ¶Institute of Biochemistry, Charité University Hospital, Humboldt University, Berlin 13353, Germany; †Gene Mapping Center, Max Delbrück Center for Molecular Medicine, Berlin 13092, Germany; ‡Department of Biochemistry, Kobe Pharmaceutical University, Higashinada, Kobe 658-8558, Japan; §Genetic Unit, Directorate General of Health Affairs, Ministry of Health, 138 Muscat, Sultanate of Oman; and ‖Max Planck Institute for Molecular Genetics, 14195 Berlin, Germany

Edited by Victor A. McKusick, Johns Hopkins University School of Medicine, Baltimore, MD, and approved May 17, 2004 (received for review January 15, 2004)

We studied two large consanguineous families from Oman with a distinct form of spondyloepiphyseal dysplasia (SED Omani type). By using a genome-wide linkage approach, we were able to map the underlying gene to a 4.5-centimorgan interval on chromosome 10q23. We sequenced candidate genes from the region and identified a missense mutation in the chondroitin 6-*O*-sulfotransferase (C6ST-1) gene (*CHST3*) changing an arginine into a glutamine (R304Q) in the well conserved 3′-phosphoadenosine 5′-phosphosulfate binding site. C6ST-1 catalyzes the modifying step of chondroitin sulfate (CS) synthesis by transferring sulfate to the C-6 position of the *N*-acetylgalactosamine of chondroitin. From the crystal structures of other sulfotransferases, it could be inferred that Arg-304 is essential for the structure of the cosubstrate binding site. We used recombinant C6ST-1 to show that the identified missense mutation completely abolishes C6ST-1 activity. Disaccharide composition analysis of CS chains by anion-exchange HPLC shows that both ΔHexA-GalNAc(6S) and ΔHexA(2S)-GalNAc(6S) were significantly reduced in the patient's cells and that ΔHexA-GalNAc(4S,6S), undetectable in controls, was elevated. Analysis of the patient's urine shows marked undersulfation of CS, in particular reduction in 6-*O*-sulfated disaccharide and an increase in the nonsulfated unit. Our results indicate that the mutation in CHST3 described here causes a specific but generalized defect of CS chain sulfation resulting in chondrodysplasia with major involvement of the spine.

Chondroitin sulfate (CS) chains are ubiquitously found as proteoglycan side chains in the extracellular matrices and at cell surfaces, and main components of cartilage consisting of repeating disaccharide units sulfated either at the C-6 or the C-4 position of the GalNAc. Sulfate groups are transferred from 3′-phosphoadenosine 5′-phosphosulfate (PAPS) by sulfotransferases, most of which have been cloned, functionally analyzed, and classified into groups depending on their substrate specificity and amino acid sequence (1). C6ST-1 catalyzes the transfer of sulfate specifically to position 6 of the GalNAc residue (2). Sulfation profiles of glycosaminoglycans (GAGs), including CS change during development (3, 4), vary with age and are considered to be important for multiple aspects of extracellular matrix function such as neurite outgrowth, lymphocyte–endothelial cell interactions, and cell signaling (5).

Disturbances in supply and utilization of sulfate cause a variety of overlapping phenotypes, many of these affecting the skeleton underscoring the importance of an appropriate degree of sulfation of CS chains in skeletal development and maintenance. For example, different mutations in the diastrophic dysplasia sulfate transporter (DTDST) gene (*SLC26A2*) (OMIM 606718) cause diastrophic dysplasia, achondrogenesis type IB, atelosteogenesis type II, and a recessive form of multiple epiphyseal dysplasia. The phenotypes cover a broad spectrum of skeletal dysplasias ranging from relatively benign conditions to severe defects incompatible with life (for review see ref. 6). Spondyloepimetaphyseal dysplasia (SEMD) Pakistani type and the mouse mutant "brachymorphic" also show undersulfation of CS chains (7) and are caused by defects in the *ATPSK2* gene (OMIM 603005), which is necessary for sulfate activation (8). Defects in both DTDST and ATPSK2 most likely result in lowering the intracellular PAPS concentration, which likely causes broad nonspecific undersulfation of CS chains present abundantly in the skeletal structure.

In this study, we identified the causal gene for the recently discovered spondyloepiphyseal dysplasia (SED) Omani type (OMIM 60837) as *CHST3* (OMIM 603799) that encodes chondroitin 6-*O*-sulfotransferase 1 (C6ST-1). SEDs belong to a genetically heterogeneous group of osteochondrodysplasias (for review see ref. 9). SED Omani type has been described as a clinical entity distinct from other SEDs based on the unique phenotype of two large consanguineous families from the sultanate of Oman (10). The recessively inherited disorder is characterized by normal length at birth but severely reduced adult height (110–130 cm), severe progressive kyphoscoliosis, arthritic changes with joint dislocations, genu valgum, cubitus valgus, mild brachydactyly, camptodactyly, microdontia, and normal intelligence. As a consequence of the arthropathy and the contractures, affected individuals develop restricted joint movement. Here we describe that the SED Omani type is associated with a mutation in a specific GAG sulfotransferase gene, in contrast to the above described dysplasias caused by deficiencies in the sulfate supply. The identified missense mutation completely abolishes C6ST-1 activity. This finding adds a clinical phenotype to the growing group of "sulfate diseases" and, more importantly, shows that defects in GAG sulfotransferases can produce a human genetic disorder.

Patients, Materials, and Methods

Patients. Nine patients from two large siblingships were included in this study. The phenotype and a detailed clinical description has been described (10). In brief, affected individuals show a distinct phenotype consisting of near normal length at birth, but severe progressive scoliosis resulting shortening of the upper segment and a final adult height of 110–139 cm. The linear growth in all patients was slower than expected in the first 6 months of life and dropped to below normal thereafter. Between 2 and 10 years of age, height was on average 20 cm (±4 SD) below the third centile but was increasing steadily parallel to the third centile. Subsequently, growth velocity deteriorated further, and this coincided with the

This paper was submitted directly (Track II) to the PNAS office.

Abbreviations: CS, chondroitin sulfate; PAPS, 3′-phosphoadenosine 5′-phosphosulfate; GAG, glycosaminoglycan; DTDST, diastrophic dysplasia sulfate transporter; SED, spondyloepiphyseal dysplasia; cM, centimorgan; LOD, logarithm of odds; ABC, ATP-binding cassette; C4ST, chondroitin-4-*O*-sulfotransferase.

**To whom correspondence should be addressed. E-mail: stefan.mundlos@charite.de.

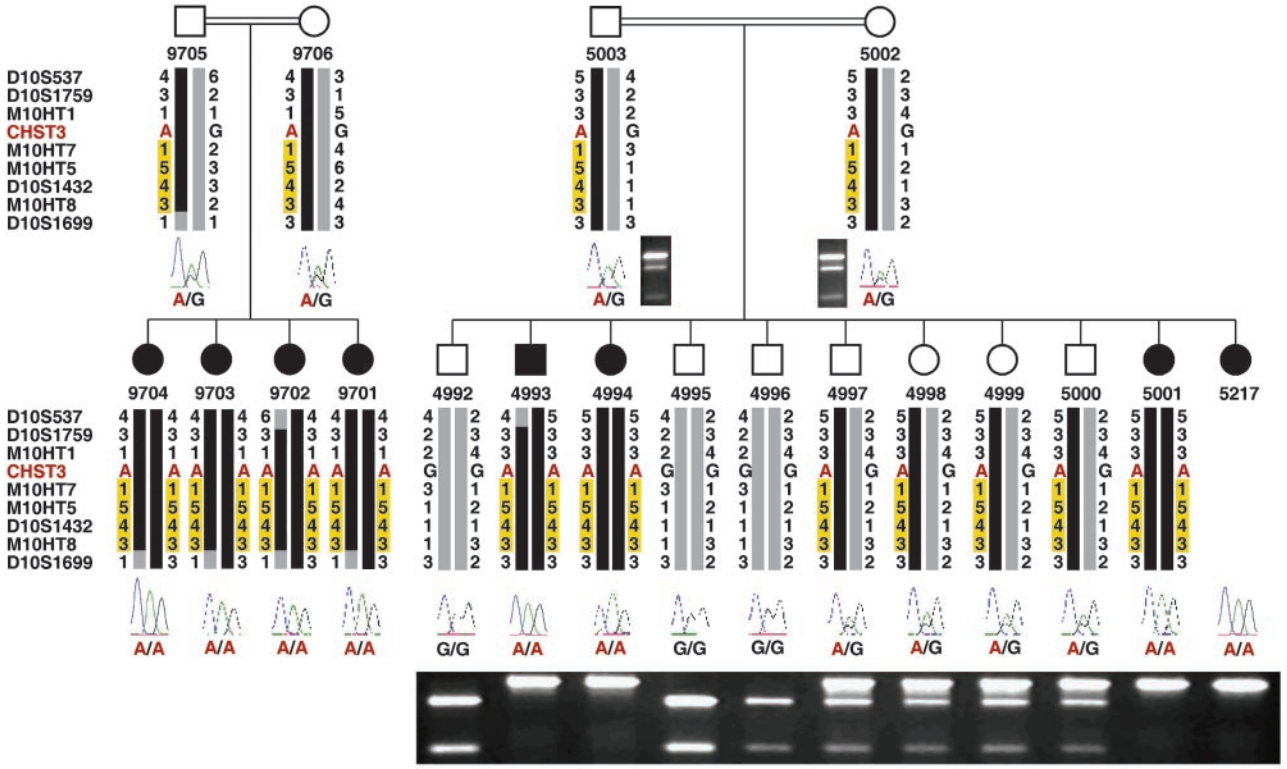

Fig. 1. Haplotype analysis for family A and B at chromosome 10q23–24 are shown for the individuals where DNA was available. Eight microsatellite markers are shown in black, and the position of the *CHST3* gene is shown in red. The order is from centromere to q-terminal using physical distances derived from National Center for Biotechnology Information (NCBI) assembly build 33. Circles denote females, squares denote males. Filled symbols indicate diagnosis of SED. Haplotypes are presented as gray and black bars. All affected people are homozygous for the affected (black) haplotype. The fragment from an ancestral founder haplotype remaining in both families is drawn as a dark yellow box. Position 911 from *CHST3* gene, carrying the G → A mutation, is presented as trace sequence picture cutout under the haplotype from each individual. Patterns of gel electrophoresis after *Sma*I restriction enzyme digest from PCR fragments covering the *Sma*I site-destroying mutation are shown for family B.

development of scoliosis. Scoliosis is preceded by diminished intervertebral discs and abnormal vertebral end plates, resulting in fusion of vertebrae. The epiphysis are small, and all large joints show severe arthritic changes with joint dislocations. The elbow, wrist, and hip joints were affected starting in infancy and showed restricted movement. The limbs show rhizomelic shortening, genu valgum, cubitus valgus, mild brachydactyly, and camptodactyly. Intelligence is normal. The progressive degenerative changes in spine and joints lead to severe physical disability in early adulthood. The pedigrees are shown in Fig. 1. Fibroblasts were grown from a skin biopsy taken from the inside of the left forearm from two of the affected family members (4993 and 4994).

Linkage Analysis. Genomic DNA was extracted from peripheral blood lymphocytes by standard procedures. A genome-wide scan with a set of 395 polymorphic microsatellite markers (modified Weber 9 set, Marshfield Institute, Marshfield, WI), with an average spacing of ≈11 centimorgans (cM) according to the Marshfield map, was performed. Additional markers were used for the fine mapping. Products of PCR assays with fluorescently labeled primers were analyzed by automated capillary genotyping on a MegaBACE 1000 (Amersham Pharmacia). A two-point logarithm of odds (LOD) score calculation was performed by using the LINKAGE 5.20 package (11) and choosing a recessive model of disease inheritance with full penetrance. Equal female and male recombination rates and a disease allele frequency for SED Omani type of 0.0001 were assumed. Haplotype reconstruction and multipoint LOD score calculation were performed by using GENHUNTER 2.1_R2 (12).

Mutation Analysis. Standard protocol PCRs were carried out to amplify all exons and flanking splice sites of the genes *P4HA1* (OMIM 176710) and *CHST3* from genomic DNA (PCR primers are available from the authors upon request). PCR products were analyzed by 2% agarose gel electrophoresis. Purified PCR products were sequenced in both directions by using the Applied Biosystems Prism BigDye terminator cycle sequencing reaction kit and PCR primers as sequencing primers. The products of the reaction were evaluated on an Applied Biosystems 3100 DNA analyzer. Because the identified mutation disrupts a *Sma*I restriction site, a restriction enzyme assay was designed to verify the mutation in the patients' DNA and exclude its presence in control samples of healthy individuals. Primers for amplification of the genomic DNA fragments were the same as for sequencing. Approximately 10 μl of PCR product were digested with 5 units of *Sma*I at 25°C for 2 h. Fragments were separated by electrophoresis on a 2% agarose gel and visualized by ethidium bromide staining.

Functional Studies. Sulfotransferase assays were carried out as described (4). We used both fibroblast homogenates derived from cell cultures of two affected individuals (4993 and 4994) and compared them to two unaffected age-matched controls. In addition to the fibroblasts, we analyzed CS chains in the urine from one of the two affected individuals (4993). We used recombinant enzymes for the determination of chondroitin sulfotransferase activity. Samples were incubated for 1 h with polymer chondroitin as a substrate (acceptor) and [^{35}S]PAPS as a cosubstrate (donor). The products were isolated by gel filtration. Subsequently, the isolated products were quantified by liquid scintillation counting. For cell lysates chondroitin sulfotransferase activities were determined in total as well as separately for chondroitin-4-*O*-sulfotransferase (C4ST) and C6ST. For determining the sulfated

Table 1. Two-point sum LOD scores for both kindreds at various recombination fractions (θ = 0–0.4) for markers of the 10q23–24 region

Marker	cM*	Mb†	LOD scores						
			0.000	0.001	0.010	0.050	0.100	0.200	0.400
D10S537	**89.16**	72.29	$-\infty$	−1.982	−0.051	1.040	1.258	1.108	0.331
D10S1759	**91.24**	72.95	3.612	3.604	3.532	3.210	2.803	1.990	0.498
M10HT1	92.68	73.43	3.185	3.179	3.121	2.858	2.523	1.831	0.450
M10HT7	93.78	74.36	2.884	2.878	2.825	2.586	2.279	1.649	0.419
M10HT5	93.85	74.43	5.229	5.219	5.123	4.693	4.145	3.022	0.783
D10S1432	**93.97**	74.56	4.991	4.981	4.887	4.464	3.926	2.824	0.639
M10HT8	94.18	75.92	3.185	3.179	3.122	2.864	2.533	1.846	0.473
D10S1699	**95.79**	78.08	−0.995	−0.283	0.591	1.089	1.146	0.957	0.281

*Marker positions in cM refer to the DECODE map (29). Original DECODE positions are shown in boldface; others refer to physical data.

†Physical positions based on National Center for Biotechnology Information (NCBI) build 33 assembly.

positions 4 and 6 of GalNAc residues, 9/10th of each ^{35}S-labeled chondroitin fraction was digested by using 5 milliunits of chondroitinase ATP-binding cassette (ABC), and the resulting unsaturated disaccharides were identified by HPLC. C4ST and C6ST activities were determined based on the [^{35}S]sulfate incorporation into ΔHexA-GalNAc(4S) and ΔHexA-GalNAc(6S), where ΔHexA, 4S, and 6S represent unsaturated hexuronic acid, 4-*O*-sulfate, and 6-*O*-sulfate, respectively. The construction of a soluble form of wild-type and mutated C6ST-1 was carried out as described (2). In brief, the first NH_2-terminal 48 amino acids of C6ST-1 were substituted by a cleavable insulin signal sequence fused to a protein A IgG-binding domain. The soluble form of C6ST-1 was secreted from transfected COS-1 cells into the medium and adsorbed on IgG-Sepharose beads to separate it from endogenous C6ST.

The fractionation and analysis of oligosaccharides were carried out by HPLC as described (4). The GAG fraction prepared from fibroblasts of two age-matched controls or affected individuals was digested with chondroitinase ABC. Each digest was labeled with 2-aminobenzamide and analyzed by anion exchange HPLC on an amine-bound silica PA-03 column (13).

Structural Modeling. The C6ST-1 model from the PAPS-binding region was created with QUANTA97 (Accelrys, San Diego) on the basis of the hydroxysteroid sulfotransferase structure (PDB ID code 1EFH) and drawn with VIEWER PRO 4.2 (Accelrys).

Results

Mapping. We performed a genome scan with a 10-cM microsatellite marker panel in a family with four siblings affected by SED and their unaffected consanguineous parents (family A). Initial evidence of linkage was obtained with marker at locus *D10S1432* (two-point LOD score of $Z_{max} = 2.408$ at $\theta = 0$), suggesting linkage to chromosome 10q23. No other regions of the genome showed any linkage to the phenotype as revealed by multipoint LOD score calculation including all markers of the scan. For further fine mapping, previously undescribed microsatellite markers, such as *M10HT1*, *M10HT5*, *M10HT7*, and *M10HT8* were developed based on the National Center for Biotechnology Information (NCBI) genomic sequence assembly data (build 32; April 2003). Fine mapping was performed including family B, a second consanguineous family with a total of four affected and seven unaffected siblings (Fig. 1), resulting in a significant two-point sum LOD score of >5.2 at $\theta = 0$ for marker *M10HT5* (Table 1). Recombination events in family A defined the borders of the disease interval at markers *D10S537* and *D10S1699*. Unfortunately, no recombinations within this interval were observed in family B. However, haplotype analysis showed clear evidence of a common founder haplotype shared by both families. The shared haplotype defined a smaller disease interval of ≈3.11 cM or 4.65 megabases (Mb) delimited by markers *M10HT1* and *D10S1699*. All affected individuals were homozygous for this haplotype, whereas unaffected individuals were either heterozygous or noncarriers (Fig. 1).

Mutation Identification. When we used the National Center for Biotechnology Information (NCBI) map viewer, we found 65 gene entries in the critical interval, including *P4HA1* (encoding for proline 4-hydroxylase) and *CHST3* (encoding for C6ST-1), which we considered as most interesting candidate genes because they are known to play a role in the modification of extracellular matrix proteins, etc. (14). The coding regions of both genes were sequenced, and a missense mutation was identified in exon 3 of *CHST3*. The gene consists of three exons, spans ≈49.2 kb of genomic sequence, and has an unusually large 3′ UTR of 5,115 bp. The ORF of 1,437 bp coding for 479 aa starts in exon 2 (Fig. 2). We identified a 911G → A base substitution resulting in an arginine to glutamine exchange (R304Q). We have found all affected individuals to be homozygous and the parents, as obligate carriers, heterozygous for this mutation. None of the healthy siblings was found to be homozygous for the mutation (Fig. 1). By an independent method using a *Sma*I restriction enzyme digestion assay, we could verify this point mutation (Fig. 1, family B).

By using sequence alignments between different species and sulfotransferase, we were able to show that R304 is located within a highly conserved region previously implicated in PAPS binding (15) (Fig. 2).

Sulfotransferase Activity of Fibroblasts. To test whether the mutation R304Q affects the sulfotransferase activity of C6ST-1, we analyzed its activity in fibroblasts obtained from one patient (4994)

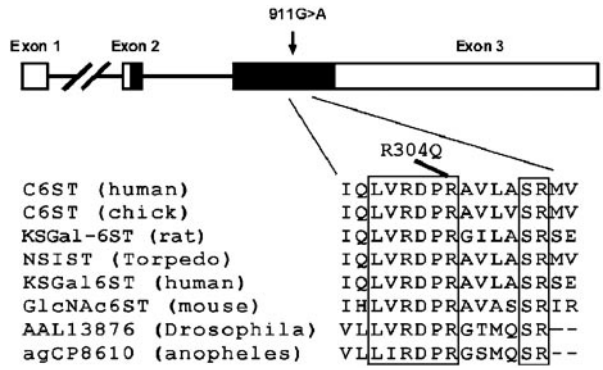

Fig. 2. *CHST3* gene structure. Black filled boxes represent coding sequence. White boxes represent untranslated regions. The arrow denotes the missense mutation 911G → A resulting in an R304Q exchange. A multiple sequence alignment is shown below demonstrating the high conservation around R304. The conserved sequence is boxed.

Table 2. Comparison of the sulfotransferase activities of fibroblast homogenates

Patient	Total activity*	C4ST activity,† nmol per mg of protein per h	C6ST-1 activity†
Control 1	16.1	3.0	13.1
Control 2	13.9	4.7	9.2
Affected individual	2.7	2.7	ND

ND, not detectable (<0.1 nmol per mg of protein per h).

*The values represent the averages of the data from two independent experiments.

†For determining the sulfated positions 4 and 6 of GalNAc residues, nine-tenths of each ^{35}S-labeled CS fraction was digested by using 5 milliunits of chondroitinase ABC, and the resulting unsaturated disaccharides were identified by HPLC as shown in Fig. 1. C4ST and C6ST-1 activities were determined based on the incorporation into ΔHexA-GalNAc(4S) and ΔHexA-GalNAc(6S), respectively.

and two unaffected control individuals. We determined the total sulfotransferase activity as well as the activity of C4ST and C6ST separately (Table 2). Very similar results were obtained for the two controls in all three parameters. In contrast, no C6ST activity and a much reduced total activity were found in the cells of the patient. Interestingly, the residual total sulfotransferase activity was equal to the C4ST activity measured for the patient, retaining ≈30% sulfation of chondroitin (Table 3).

Testing of Recombinant Sulfotransferase Activity. For testing recombinant mutated sulfotransferase activity, soluble variants of C6ST-1 were cloned, expressed, purified, and assayed as described in *Patients, Materials, and Methods*. R304Q-mutated C6ST-1 did not show any detectable activity, whereas wild-type C6ST-1 activity was as high as 146.7 pmol per ml of medium per h (Table 4). Equal expression of both recombinant enzymes was checked by Western blot analysis (data not shown).

Disaccharide Composition of Fibroblast CS Chains. To obtain evidence that deficiency of C6ST-1 results in an altered chondroitin sulfation pattern, we performed a disaccharide composition analysis of CS chains by anion-exchange HPLC after digestion with chondroitinase ABC. We compared various sulfated disaccharides from fibroblasts of two controls and two affected individuals. No major differences between controls 1 and 2 were detected (Table 3 and Fig. 3). The sum of the signals amounted to 1,391 pmol/mg for control 1, 899 pmol/mg for control 2, and 2,249 and 3,346 pmol/mg for the two affected individuals. For control 1, ΔHexA-GalNAc(6S) and ΔHexA(2S)-GalNAc(6S) were detected at levels of 230 and 21 pmol/mg, respectively; for control 2, values of 121 and 13 pmol/mg were determined for the two disaccharides, whereas the values were

Table 4. Comparison of the sulfotransferase activities of the recombinant wild-type C6ST-1 and R304Q C6ST-1 in transfected COS-1 cells

C6ST-1 variant	Activity, pmol per ml of medium per h
Mock	ND
Wild-type C6ST-1	146.7
R304Q C6ST-1	ND

ND, not detectable (<1.0 pmol per ml of medium per h). The values represent the averages of the date from two independent experiments.

65 and 14 pmol/mg in the cells of affected individual 4994 and 23 and 15 pmol/mg in affected individual 4993. On the other hand, no signal for ΔHexA-GalNAc(4S,6S) was detected for the controls, but 52 and 60 pmol/mg of this disaccharide was measured in the affected individuals. The ratios of ΔHexA-GalNAc to ΔHexA-GalNAc(4S) were similar in controls and patients (Table 3).

Disaccharide composition analysis of urinary CS (Table 5) showed a reduction of ΔHexA-GalNAc(6S) (1.1 pmol/mg) in the patient when compared to controls (34.4 and 25.1 pmol/mg) and an elevation of ΔHexA-GalNAc (21.4 in the patient vs. 12.5 and 10.5 in the controls).

Model of the C6ST-1 Active Site. The overall sequence homology between the two classes of sulfotransferases, the cytosolic enzymes and the Golgi membrane enzymes, is quite low. Nevertheless, there are two regions in the vicinity of the binding site of the cosubstrate PAPS where there is some more significant sequence homology: the regions 141–147 (human C6ST numbering) and 295–309. The first region is in contact mainly with the adenine moiety via Phe-147 and contains the putative catalytic residue Arg-142; the second contributes to the PAPS-binding site by interactions of Arg-301 and Ser-309 with the 3′-phosphate of PAPS. Arg-304, which is substituted by Gln in the mutant enzyme, is part of this region, but its side chain points in a direction just opposite the bound PAPS. In the reported crystal structures of sulfotransferases, the guanidine group of this residue forms a salt bridge with a conserved aspartic acid residue (Asp-267 in hydroxysteroid sulfotransferase, Asp-277 in estrogen sulfotransferase, PDB ID code 1AQU, Asp-277 in sulfotransferase SULT1A1, PDB ID code 1LS6) or glutamic acid (Glu-332 in retinol DH, PDB ID code 1FMJ), and forms a hydrogen bridge with the neighboring Asn-302 (Asp-122 in estrogen sulfotransferase). There is not much sequence homology with C6ST in this region (except Pro-123, which corresponds to Pro-303 in C6ST), making it difficult to identify the corresponding surrounding of Arg-304 in C6ST, but there should be a similar hydrophobic cluster. In all of these structures, the nonpolar part of the Arg side chain is surrounded by a well defined cluster of hydrophobic residues (Pro-123, Trp-254, Phe-258, and Phe-266 in estrogen sulfotransferase). Obviously, the arginine side chain seems

Table 3. Disaccharide composition analysis of CS produced by fibroblasts from patients and control subjects

	CS disaccharide composition,* pmol (%)			
	Control 1	Control 2	Affected individual 1	Affected individual 2
ΔHexA-GalNAc	167 (12.0)	103 (11.5)	391 (17.4)	264 (7.9)
ΔHexA-GalNAc(6S)	230 (16.6)	121 (13.4)	65 (2.9)	23 (0.7)
ΔHexA-GalNAc(4S)	973 (69.9)	662 (73.7)	1,727 (76.8)	2,984 (89.2)
ΔHexA(2S)-GalNAc(6S)	21 (1.5)	13 (1.4)	14 (0.6)	15 (0.4)
ΔHexA-GalNAc(4S,6S)	ND	ND	52 (2.3)	60 (1.8)
Total	1,391 (100)	899 (100)	2,249 (100)	3,346 (100)

Values represent the averages of three independent experiments each performed in duplicate and are expressed as pmol (%) of disaccharides per mg of protein of the fibroblasts. ND, not detectable.

*Signal number according to notation in Fig. 3.

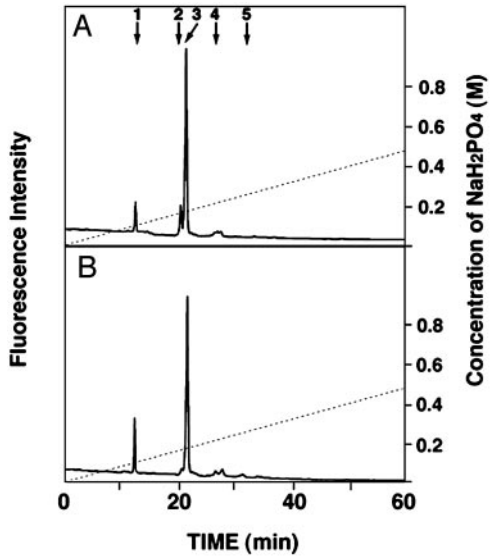

Fig. 3. Disaccharide composition analysis of CS chains produced by fibroblasts from a patient (4493) and a control subject. The GAG fraction prepared from fibroblasts of age-matched control 1 (*A*) or affected individual (*B*), respectively, was digested with chondroitinase ABC. Each digest was labeled with 2-aminobenzamide and analyzed by anion-exchange HPLC on an amine-bound silica PA-03 column (2). The elution positions of authentic 2-amino-benzamide-labeled disaccharide standards derived from CS are indicated by numbered arrows in *A*. 1, ΔHexA-GalNAc; 2, ΔHexA-GalNAc(6S); 3, ΔHexA-GalNAc(4S); 4, ΔHexA(2S)-GalNAc(6S); 5, ΔHexA-GalNAc(4S,6S).

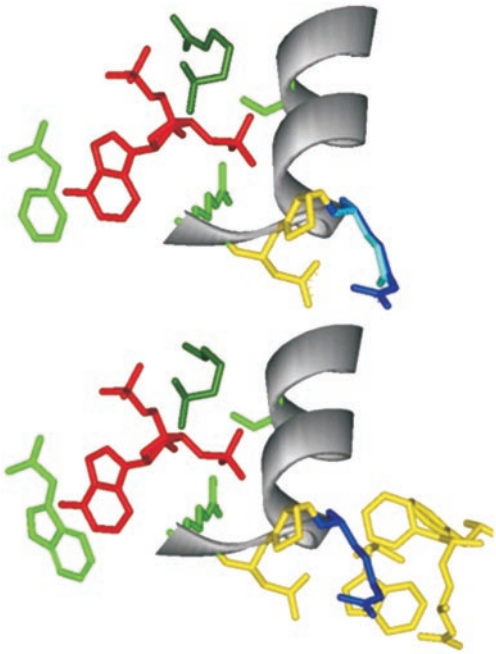

Fig. 4. Schematic representation of the PAPS-binding region of human C6ST-1 (model) (*Upper*) and human hydroxysteroid sulfotransferase (HST) (PDB ID code 1EFH) (*Lower*). Arg-142 (Lys-44) supposed to be involved in catalysis is shown in dark green; important residues in contact with PAPS [Phe-147 (Trp-49), Arg-301 (Arg-121), and Ser-309 (Ser-129)] are shown in light green, Arg-304 (Arg-124) (shown in blue) is converted to Gln (shown in light blue) in the mutant C6ST enzyme; residues surrounding Arg-304 (Arg-124) are shown in yellow [Asn-302 (Asp-122), Pro-303 (Pro-123), (Trp-254), (Phe-258), (Phe-266), and (Asp-267)]; PEPS is shown in red; secondary structure is shown in gray. Residue numbering for HST is given in parentheses.

to be of special importance for the stabilization of this helical part of the sulfotransferase structure, which contributes to the PAPS-binding site and thus to a proper orientation of the cosubstrate. This may explain the loss of activity with Gln instead of Arg at this position in C6ST-1. Fig. 4 shows a schematic representation of the PAPS-binding region from C6ST-1 and hydroxysteroid sulfotransferase.

Discussion

The data represented here provide strong evidence that SED Omani type is caused by a missense mutation in *CHST3*, the gene encoding C6ST-1. *In vitro*, the enzyme accepts different substrates (chondroitin, various CS variants, keratan sulfate, sialyl lactosamine oligosaccharides) with major specificity for chondroitin (2). C6ST-1 is anchored by its transmembrane domain in the Golgi apparatus. Human C6ST-1 exhibits an abundant expression in the adult heart, placenta, skeletal muscle, and thymus in contrast to very little expression in adult lung and peripheral blood leukocytes (16). For the chicken brain, a developmentally regulated expression of this enzyme and the reaction products was reported (4). In the mouse, C6ST-1 was found in spleen and lung but also in eye, stomach, ovary, kidney, and, dependent on the developmental stage, in brain (17). Recently, the function of C6ST-1 has been further elucidated by inactivating *CHST3* in the mouse (18). *CHST3*$^{-/-}$ mice were born at the expected frequency and were viable through adulthood. No apparent differences between normal and knockout mice were reported, and histological sections of the cerebral cortex revealed normal organization. Differences were only found with respect to lower numbers of naive T lymphocytes in the spleen of *CHST3*$^{-/-}$ mice (18). Considering SED Omani type patients as functionally deficient in C6ST-1, it remains unclear why humans develop exclusively a skeletal phenotype despite the widespread expression of C6ST-1 in different tissues and why there are obvious differences between mouse and human in the consequences of the enzyme deficiency. Erect position causes a mechanical stress, which might have manifested the phenotypes in the spine observed in human but not in mouse.

Table 5. Disaccharide composition analysis of urinary CS from the patient and the control subjects

	CS disaccharide composition, pmol (%)		
	Control 1	Control 2	Affected individual 1
ΔHexA-GalNAc	12.5 (11.2)	10.5 (15.4)	21.4 (28.2)
ΔHexA-GalNAc(6S)	34.4 (30.7)	25.1 (36.8)	1.1 (1.5)
ΔHexA-GalNAc(4S)	57.4 (51.2)	29.0 (42.6)	49.9 (65.6)
ΔHexA(2S)-GalNAc(6S)	1.7 (1.5)	1.1 (1.7)	0.1 (0.1)
ΔHexA(2S)-GalNAc(4S)	1.2 (1.1)	0.4 (0.6)	1.0 (1.2)
ΔHexA-GalNAc(4S,6S)	4.7 (4.3)	2.0 (2.9)	2.4 (3.1)
ΔHexA(2S)-GalNAc(4S,6S)	ND	ND	0.1 (0.1)
Total	111.9 (100)	68.1 (100)	76.0 (100)

Values represent the averages of three independent experiments each performed in duplicate and are expressed as pmol (%) of disaccharides per mg of creatinine of urine. ND, not detectable.

Analysis of disaccharide composition of CS chains produced by fibroblasts from SED patients revealed some interesting findings. Signals of ΔHexA-GalNAc(6S) and ΔHexA(2S)-GalNAc(6S) were significantly reduced. The proportion of 6-*O*-sulfated disaccharide unit markedly decreased, but not to zero, which may be attributable to chondroitin 6-*O*-sulfotransferase 2 (19). Disaccharide composition analysis from urine revealed similar findings, with a strong reduction in the ΔHexA-GalNAc(6S) and an increase in the nonsulfated unit (Table 5). These results are in agreement with our findings in cell transfection experiments using mutated enzyme constructs and C6ST activity measurements in fibroblasts from

affected individuals. We also found a minor signal of ΔHexA-GalNAc(4S,6S) in the patients, which was absent from two controls. We assume this to be the result of an elevated *N*-acetylgalactosamine-4-*O*-sulfate 6-*O*-sulfotransferase (GalNAc4S-6ST) activity (20). It has been speculated that GalNAc4S-6ST is involved in the formation of nonreducing terminal GalNAc(4S,6S) residues found in CS chains (20). In our patients, this enzyme may partially fill the gap created by the loss of C6ST-1 function. Surprisingly, the total amount of disaccharides in the tested patient was twice as high as in the controls. Although the sample size is too small to draw a definite conclusion from this finding, it may point to a compensatory induction of CS or disturbances in the control of CS expression. Furthermore, our results obtained in fibroblasts and urine may not fully reflect the consequences of the mutation on cartilage matrix proteins, because it cannot be ruled out that other 6-*O*-sulfotransferases present in cartilage, but not in fibroblasts, partially compensate for the lack of C6ST-1.

Brachyolmia refers to a rare group of osteochondrodysplasias characterized clinically by short-trunk dwarfism and radiologically by generalized platyspondyly without significant long-bone abnormalities (21). In patients with the Toledo subtype (OMIM 271630) of this dysplasia, an undersulfated chondroitin 6-*O*-sulfate (CS-C) was shown to be excreted in the urine, suggesting a possible defect in a chondroitin sulfotransferase (22). In particular, a high proportion of nonsulfated disaccharides, an abnormally low proportion of 6-*O*-sulfated disaccharides of the CS chains in the urine, and a low sulfotransferase activity in the serum were detected. Subsequently, a second individual with similar clinical and biochemical findings was reported by Sewell *et al.* (23). However, no mutation has been identified so far. SED Omani (10) and brachyolmia Toledo type are clinically distinct conditions with major differences in the phenotype as well as clinical severity. Whereas SED Omani type shows severe involvement of the epiphyses, osteoarthrosis, and joint contractures, the Toledo type of brachyolmia is restricted to the spine and shows no involvement of long bones. Furthermore, the dental abnormalities seen in SED Omani type patients were not described in patients with Toledo type brachyolmia. However, both conditions exhibit abnormalities of the spine with platyspondyly and narrowing of the intervertebral space. It is thus conceivable that both conditions are allelic or that their respective genes function within the same pathway, with SED Omani type representing the severe end of the spectrum.

The importance of an appropriate degree of sulfation of CS chains for the integrity and function of cartilage has been demonstrated by identifying other genetic diseases affecting sulfation. In 1998, the molecular basis of spondyloepimetaphyseal dysplasia (SEMD) Pakistani type was identified and was shown to be caused by the same gene defect as the brachymorphic mouse (24). The affected gene, *ATPSK2*, codes for a bifunctional single enzyme protein ATP synthase harboring both ATP sulfurylase and APS kinase and is involved in the synthesis of the active sulfate PAPS (7), which serves as a cosubstrate for sulfotransferases like C6ST-1. SEMD Pakistani type (OMIM 603005.0001) shows some phenotypic overlap with the condition described here, including reduced disk spaces in the lumbar and thoracic region, platyspondyly, and irregular end plates (25). Sulfate is transported via a specific transporter into the cell. Mutations in the sulfate transporter gene *DTDST* were shown to produce a spectrum of osteochondroplasias with characteristic, overlapping phenotypes (6). Although the clinical picture of these conditions is distinct from SED Omani type, they do exhibit some common features, suggesting a shared pathogenetic pathway. Joint contractures, a typical feature of diastrophic dysplasia, and major spinal involvement are clearly a common feature, and thus appear to be the hallmarks of sulfation defects in the skeleton.

It should be emphasized that defects in ATPSK2 and DTDST cause lowering concentrations of intracellular sulfate and PAPS, which likely results in broad nonspecific undersulfation of CS chains abundantly synthesized in cartilage. In contrast, defects in specific GAG sulfotransferases cause severe characteristic phenotypes, as has been demonstrated for the knockout mice generated by disrupting heparan sulfate- and heparin-synthesizing sulfotransferases (26). Nonetheless, no human genetic disorder caused by a defect in a GAG sulfotransferase has been reported. Although human macular corneal dystrophies type I and type II have been identified to be caused by mutations in the *N*-acetylglucosamine-6-*O*-sulfotransferase gene *CHST6* expressed in cornea (27), the sulfation defects involve an atypical GAG keratin sulfate without uronic acid. Substrate specificity and regulation of tissue-specific expression is likely to account for such distinct phenotypes.

Intriguingly, the CS chains from the patients' fibroblasts showed a comparable degree of sulfation to the control (Table 3), suggesting that 6-*O*-sulfation is of particular importance for chondrocyte differentiation and bone development. Furthermore, the severe spinal involvement and the narrowing of the intervertebral discs suggest an essential role for 6-*O*-sulfated CS chains in the development and maintenance of these structures. In this regard, it is of special interest to investigate whether a specific oligosaccharide sequence including a 6-*O*-sulfate group is required for any functional protein ligand in the spine, as in the case of the recognition of specific sulfated tetrasaccharide sequences by chemokines and L- and P-selectins (28). *CHST3* should be considered a candidate gene for other, more common conditions involving the spine and intervertebral discs, such as idiopathic scoliosis or spondylolisthesis.

This work was supported by a grant from the Deutsche Forschungsgemeinschaft (to S.M.) and by Federal Ministry for Research and Education Grant 01 GR 0104 (to P.N.). The work at Kobe Pharmaceutical University was supported in part by the Scientific Research Promotion Fund of the Japan Private School Promotion Foundation, a Grant-in-Aid for Scientific Research, and the National Project on Functional Glycoconjugate Research Aimed at Developing New Industry from the Ministry of Education, Science, Sports, and Culture of Japan.

1. Sugahara, K. & Kitagawa, H. (2000) *Curr. Opin. Struct. Biol.* **10,** 518–527.
2. Tsutsumi, K., Shimakawa, H., Kitagawa, H. & Sugahara, K. (1998) *FEBS Lett.* **441,** 235–241.
3. Kimata, K., Okayama, M., Ooira, A. & Suzuki, S. (1973) *Mol. Cell Biochem.* **1,** 211–228.
4. Kitagawa, H., Tsutsumi, K., Tone, Y. & Sugahara, K. (1997) *J. Biol. Chem.* **272,** 31377–31381.
5. Sugahara, K., Mikami, T., Uyama, T., Mizuguchi, S., Nomura, K. & Kitagawa, H. (2003) *Curr. Opin. Struct. Biol.* **13,** 612–620.
6. Rossi, A. & Superti-Furga, A. (2001) *Hum. Mutat.* **17,** 159–171.
7. Sugahara, K. & Schwartz, N. B. (1979) *Proc. Natl. Acad. Sci. USA* **76,** 6615–6618.
8. ul Haque, M. F., King, L. M., Krakow, D., Cantor, R. M., Rusiniak, M. E. M. & Cohn, D. H. (1998) *Nat. Genet.* **20,** 157–162.
9. Kornak, U. & Mundlos, S. (2003) *Am. J. Hum. Genet.* **73,** 447–474.
10. Rajab, A., Kunze, J. & Mundlos, S. (2004) *Am. J. Med. Genet.* **126A,** 413–419.
11. Lathrop, G. M. & Lalouel, J. M. (1984) *Am. J. Hum. Genet.* **36,** 460–465.
12. Kruglyak, L., Daly, M. J., Reeve-Daly, M. P. & Lander, E. S. (1996) *Am. J. Hum. Genet.* **58,** 1347–1363.
13. Kinoshita, A. & Sugahara, K. (1999) *Anal. Biochem.* **269,** 367–378.
14. So, C. L., Kaluarachchi, K., Tam, P. P. & Cheah, K. S. (2001) *Osteoarthritis Cartilage* **9,** Suppl. A, S160–S173.
15. Habuchi, O. (2000) *Biochim. Biophys. Acta* **1474,** 115–127.
16. Fukuta, M., Kobayashi, Y., Uchimura, K., Kimata, K. & Habuchi, O. (1998) *Biochim. Biophys. Acta* **1399,** 57–61.
17. Uchimura, K., Kadomatsu, K., Fan, Q. W., Muramatsu, H., Kurosawa, N., Kaname, T., Yamamura, K., Fukuta, M., Habuchi, O. & Muramatsu, T. (1998) *Glycobiology* **8,** 489–496.
18. Uchimura, K., Kadomatsu, K., Nishimura, H., Muramatsu, H., Nakamura, E., Kurosawa, N., Habuchi, O., El-Fasakhany, F. M., Yoshikai, Y. & Muramatsu, T. (2002) *J. Biol. Chem.* **277,** 1443–1450.
19. Kitagawa, H., Fujita, M., Ito, N. & Sugahara, K. (2000) *J. Biol. Chem.* **275,** 21075–21080.
20. Ohtake, S., Ito, Y., Fukuta, M. & Habuchi, O. (2001) *J. Biol. Chem.* **276,** 43894–43900.
21. Shohat, M., Lachman, R., Gruber, H. E. & Rimoin, D. L. (1989) *Am. J. Med. Genet.* **33,** 209–219.
22. Toledo, S. P., Mourao, P. A., Lamego, C., Alves, C. A., Dietrich, C. P., Assis, L. M. & Mattar, E. (1978) *Am. J. Med. Genet.* **2,** 385–395.
23. Sewell, A. C., Wern, C. & Pontz, B. F. (1991) *Clin. Genet.* **40,** 312–317.
24. Kurima, K., Warman, M. L., Krishnan, S., Domowicz, M., Krueger, R. C., Jr., Deyrup, A. & Schwartz, N. B. (1998) *Proc. Natl. Acad. Sci. USA* **95,** 8681–8685.
25. Ahmad, M., Haque, M. F., Ahmad, W., Abbas, H., Haque, S., Krakow, D., Rimoin, D. L., Lachman, R. S. & Cohn, D. H. (1998) *Am. J. Med. Genet.* **78,** 468–473.
26. Kusche-Gullberg, M. & Kjellen, L. (2003) *Curr. Opin. Struct. Biol.* **13,** 605–611.
27. Akama, T. O., Nishida, K., Nakayama, J., Watanabe, H., Ozaki, K., Nakamura, T., Dota, A., Kawasaki, S., Inoue, Y., Maeda, N., *et al.* (2000) *Nat. Genet.* **26,** 237–241.
28. Kawashima, H., Atarashi, K., Hirose, M., Hirose, J., Yamada, S., Sugahara, K. & Miyasaka, M. (2002) *J. Biol. Chem.* **277,** 12921–12930.